Evaluation of a novel tracking system in a breathing lung model

Kilian O'Donoghue-*Student IEEE Member*, Alberto Corvó, Pietro Nardelli, Conor O' Shea, Kashif Ali Khan, Marcus Kennedy and Padraig Cantillon-Murphy, *Senior IEEE Member*

***Abstract*—We present the evaluation of an electromagnetic position tracking system for use with virtual bronchoscopy systems. Our system utilises a planar magnetic coil array and commercially available search coil sensors. Experimental results show the EM tracking accuracy to be in the range of 1-1.5mm, which is comparable to both commercial and research systems. The use of a bench-top breathing lung model is used to verify system operation in the in vitro setting. A novel fiducial-free registration method is implemented to reduce errors resulting from inaccurate landmark identification commonly associated with point-based registration. After registration, there is good agreement between the measured position of the sensor probe during endoscopic navigation and the lung airways as visualised in a 3D model of the phantom.**

I. Introduction

Electromagnetic (EM) position tracking systems have become a critical component in many minimally invasive surgical techniques [1], [2]. Commercially available systems such as NDI's Aurora and Ascension's trakSTAR are commonly used for this purpose, although various custom research based systems have also been developed [3], [4]. We have developed a novel EM tracking system that has the advantage of low cost manufacturing and an open source, customisable design [5].

Our work has demonstrated the design and operation of our system in bench top tests measuring accuracy in an ideal environment [5]. Our end application is automated navigation and virtual endoscopy in the lung. For this purpose we have evaluated our system in a breathing lung phantom. By testing in an in-vitro scenario with the associated complications of breathing, registration errors and instrument distortion, the full capability of the system can be assessed.

II. System Overview

A. EM Tracker

The system uses planar magnetic coils transmitting low frequency magnetic fields (<30 kHz) and implemented on printed circuit board (PCBs), as well as a miniature pick-up coil sensors (8mm in length, 0.5mm diameter) placed at the distal end of a catheter. By measuring induced voltage in the pick-up coil caused by an array of magnetic sources emitting at various frequencies, position and orientation can be determined by solving a non-linear system of equations [5]. Each coil is driven simultaneously at different frequencies and each signal component is separated using synchronous demodulation. Air and tissue do not affect the system due to the low frequency of operation.

A NI-6212 USB data acquisition (DAQ) card is used to sample the voltages induced in the sensor which is then loaded into Matlab (Mathworks Corp., Natick, MA) for processing. The software filters and demodulates the input signals and calculates the position and orientation. The sensor position is updated at a rate of approximately 25Hz. Commercially available sensors from NDI were used in this system. Having a fully custom EM tracking system allows for flexibility in its integration into the final system goal of automated airway navigation with virtual visualisation.

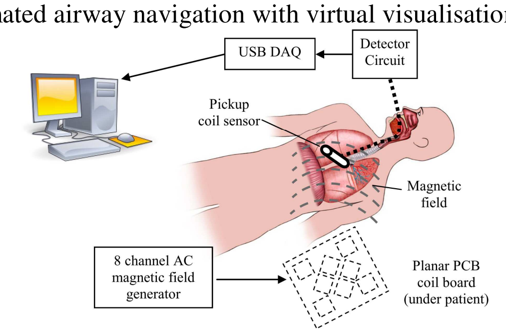

Fig. 1. An overview of the entire system. A set of magnetic coils placed below a patient generate an AC magnetic field which is detected by a sensor. This sensor voltage is sampled with a USB Data Acquisition (DAQ) unit which in turn is processed on a PC to determine an estimate of the sensor's position [5].

B. Emitter Board

The magnetic field emitter is a planar formation of PCB coils encapsulated in a 32cm×32cm×2cm Perspex housing as seen in Figure 2. An approximate working volume of 30cm×30cm×30cm where the system operates to a high degree of accuracy exists on either side of the board. For calibration of the system, a Duplo Lego board was directly mounted over the emitter. By recording a number of test points in the working volume, a set of calibration factors for each coil may be calculated.

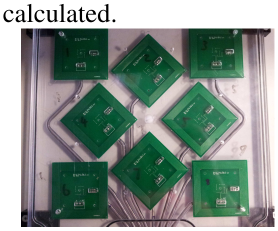

Fig. 2. The magnetic field emitter board. Eight PCB emitter coils are encapsulated in Perspex housing. The current in each coil is controlled using a constant AC current driver circuit.

C. Breathing lung model

A BioQuest Inflatable Lung kit (Nasco, Fort Atkinson, WI) was used as a phantom for evaluating the EM tracking

K. O'Donoghue, A. Corvó, P. Nardelli, C. O'Shea and P. Cantillon-Murphy are with the School of Engineering, University College Cork, Cork Ireland. (phone: 00353-21490-3727; fax: 00353-21490-1698; e-mail: kilianod@ rennes.ucc.ie).

Dr. M. Kennedy and Dr. K. A. Kahn are with Cork University Hospital, Cork, Ireland.

system. These kits comprise of plasticised pig lungs and can be inflated to various levels as required. The lungs are placed in a vacuum chamber, with the trachea connected to atmospheric pressure. When the chamber is evacuated, the pressure differential between the outside and the inside of the lungs causes them to inflate. Venting the chamber to the atmosphere equalises the pressure which causes the lungs to collapse to an uninflated equilibrium form (see Figures 3 and 4). The lungs were made to inflate and deflate in a programmable way to simulate standard breathing patterns. An Arduino Uno microcontroller was used to enable a set of solenoid valves (AD612 by CS Fluid Power) to control the lung inflation level. One valve connects the vacuum pump, while another is used for venting the chamber as seen in Figure 3. To set the breathing cycle, two dials are connected to the microcontroller. One sets the overall period of the cycle while a second sets the inflation time as a percentage of the period.

This simple and low cost solution proved very effective in simulating the human breathing pattern. A CT scan (0.65mm resolution) of the lungs in the inflated state was used to generate a 3D model [6] of the main airways which was then used to visualise the sensor's position in 3D. A custom segmentation algorithm was used to generate the 3D model.

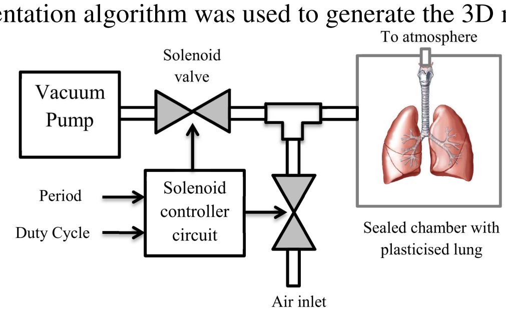

Fig. 3. Lung breathing apparatus. A set of solenoid valves are used to control the pressure in a sealed vessel. A transistor circuit controlled by a microcontroller is used to enable each valve in sequence to replicate the human breathing cycle.

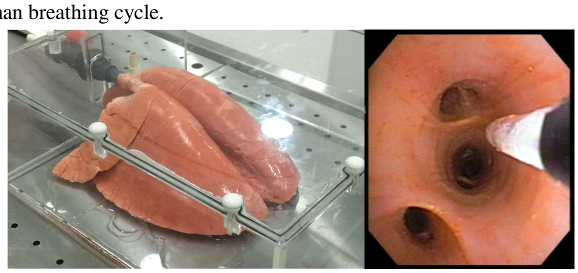

Fig. 4. (a) Plasticised pig lung when fully inflated. (b) View from the bronchoscope inside the phantom with the sensor extended out from the instrument port.

D. Bronchoscope

An Olympus 1T160 bronchoscope was used for the breathing lung tests. The unit has a 6mm OD with an instrument channel diameter of 2.8mm. The position tracking probe was inserted through the bronchoscopes instrument channel for the tests that follow.

III. Methods

A. Registration

Numerous methods exist for registration of the coordinate frame of a tracking system and that of the underlying 3D models including basic point based approaches where natural landmarks inside the real model are visually identified [7]. Other methods include the use of external fiducials and video registration [8].

Our registration algorithm is a hybrid between the iterative closest point (ICP) algorithm [9] and the in-volume maximization (IVM) algorithm [10]. ICP minimizes the distance between a number of test points inside the model to the centre line of the model. IVM attempts to minimize the number of points that are outside the model, (i.e. those which are located outside the bounds of the airway).

In our system, the coordinate frame of the EM tracker is denoted by $\mathbf{T}_e$ and the 3D model frame $\mathbf{T}_m$. The aim of registration is to find the transformation matrix $\mathbf{T}_m^e$ which minimizes the distance between a cloud of test points denoted by X_i distributed along the airway and the points that form the centre line of the airway Y_i. The number of points outside the model, X_i^{out} must also be minimised. By calculating the mean of the minimum Euclidean distance between X_i and Y_i as a function of a transformation matrix $\mathbf{T}$, a non-linear 6 variable equation results (3 each for rotation and translation) where

$$\mathbf{T}_m^e = \min_{\mathbf{T}} \left| \mathbf{T}X_i - Y_i \right|$$

This function has numerous local minima. To determine which solution is correct, the number of points outside the model is considered. If a high percentage of test points are found to be outside the 3D model, the equation solver is reset to a different starting point until the global minimum is found. To help the algorithm to converge faster, an initial registration is carried out by matching a number of test points (at least 3) to landmarks in the lung such as the carina and certain branch points. This acts as a starting point for the algorithm. This algorithm was implemented in Matlab and typical runtime was 1-2 minutes depending on the number of test points and the accuracy of the initial registration.

B. Accuracy tests

The first set of tests to verify the system accuracy involved a static 6×6×6 grid of test points in a volume of 190.5mm×190.5mm×172.8mm. At each test point, the sensor was aligned in three different directions, x, y, z which resulted in 648 points in total.

A second method to verify the accuracy of the system used the "scribble test" approach [11]. In that work, a methodology is described to verify the accuracy of position tracking systems based only on errors in a single direction away from a horizontal plane. The method involves moving a sensor around on a fixed 2D plane in a "scribble" motion and collecting numerous data points. The distance error between the predicted plane and calculated plane is then calculated [5].

C. Breathing lung phantom tests

The system operation was accessed in the breathing lung phantom. Firstly the lung was fully inflated in order to match the 3D model derived from the CT scan. In this position, the bronchoscope was used to navigate the airways. The position sensor probe was inserted inside the instrument channel and extended beyond the scope. Position data was gathered during navigation and used to register the 3D model to the EM tracker frame of reference. A simple point based registration was first used to align the coordinate frames followed by our registration algorithm. Only points gathered along the main airways are considered for the registration algorithm.

Following registration, the airways adjacent to the primary airways were navigated. This resulted in a points cloud that corresponds to the airway beyond the bounds of the 3D model. This is shown in Figure 6 (b).

For the final test, cyclic breathing was enabled. The breathing cycle period was set to 5.3s, inhalation was enabled for 27% of this period, and exhalation occupied the remaining 73%. To assess the effect of breathing, the sensor was positioned in a number of points within the lung and its displacement versus time recorded.

IV. Results

A. Bench top tests

The static position sensor tests resulted in an overall RMS error or 1.2mm and an orientation error of 1°. When all the data from the scribble tests are considered (8000 test points) the mean Z error was found to be 0.8mm with a standard deviation of 1.3mm. However if we consider only values within the 95th percentile, this error decreases to 0.6mm with a standard deviation of 0.6mm [5].

B. Registration

Figure 5 shows an example of the registration algorithm in operation. A set of test points were generated within the airway and transformed out of the airway to simulate incorrect registration. The mean distance to the centreline in this case is 7.98mm with 57/174 points inside the airway, after applying the registration algorithm detailed in the previous section the mean distance decreases to 3.67mm with 173/174 points now within the airway.

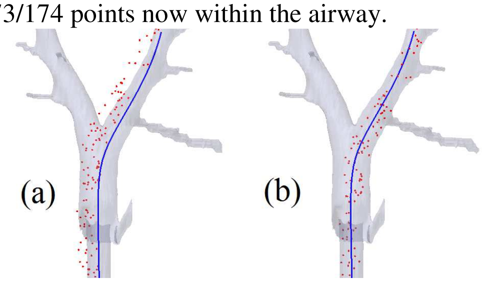

Fig. 5. Simulated performance of the registration algorithm when applied to a 3D segmented lung model. The algorithm minimises the distance between each test point and the center line as seen in the figure. (a) shows the point alignment before applying the algorithm and (b) shows the resulting transformed data set.

When applied to real data acquired within the lung, the registration algorithm reached a converged result in 53s with 80 data-points. 78/80 of these points where found to be within the airway, with a mean distance between the points and the centreline of 2.1mm.

C. Navigation accuracy

Figure 6(a) shows a plot of data points recorded when the lung was fully inflated after they have been adjusted using the registration transformation. Figure 6(b) shows points recorded beyond the lung model airways. Clearly some recorded points diverge from the 3D model. The primary reason for this is misalignment of the lung model from the initial CT scan. This might be rectified with careful position fixing of the lung in order to align it with the CT data. Other factors that affect accuracy are the level of inflation and general wear and tear of the model over time (CT data was acquired some time prior to the experiment). The errors associated with the EM tracker are small in comparison with the large divergence seen from the data.

If we consider the data gathered along the main airways (Figure 6(a)) after registration, 89.3% of the points are found to be inside the lung model.

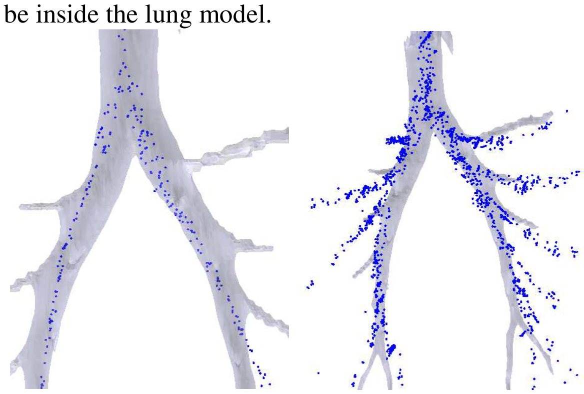

Fig. 6. (a) Overlay of points gathered during navigation of main airway after registration. (b) Plot of points beyond airway model. Erroneous points outside the model are due to positioning errors of the inflated lung model relative to the CT scan data.

In order to visually confirm registration, the sensor position was displayed in real time on the 3D model alongside the view from the bronchoscope [6]. After registration, the probe was navigated through the airways and the sensor could be seen to be invariably within the model boundary. This is shown in Figure 7. A video link to the navigation testing is available at http://youtu.be/nXWdEZ1eUlA .

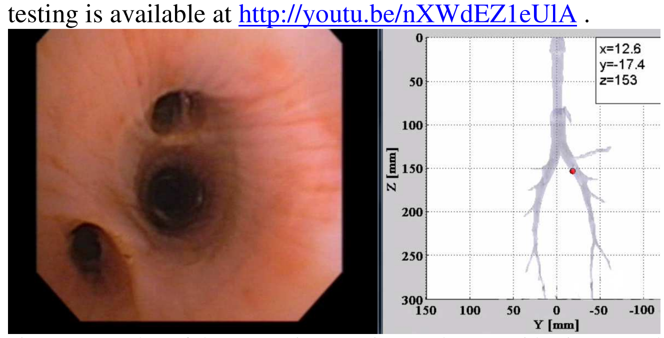

Fig. 7. Screenshot of the system in operation. Endoscope video is captured and displayed on the computer alongside a Matlab display showing the 3d lung model and the calculated position (indicated with a red dot).

D. Breathing motion

Figure 8 demonstrates position tracker displacement experienced at various points within the lung when a standard breathing cycle is implemented. As expected, the amplitude of displacement varies depending on the position of the lung. Maximum displacement was observed at points more central to the lung model, while distal points and smaller airways experienced less. The amplitude of the displacements recorded where found to range from a few mm to less than 10mm. This is in line with clinical test data from patients reported elsewhere [12], [13]. Figure 9 shows each vector component of the displacement versus time. We can see that the maximum displacement is observed in the Z direction, which represents a vertical motion. This result is expected as when the lungs inflate they expand up and outwards.

Methods exist for counteracting the effect of breathing displacements in position data [12] and future work will attempt to implement modelled displacements to account for these variations. This is required, as typically only a static 3D model is available and breathing artefacts can affect registration and overall system accuracy.

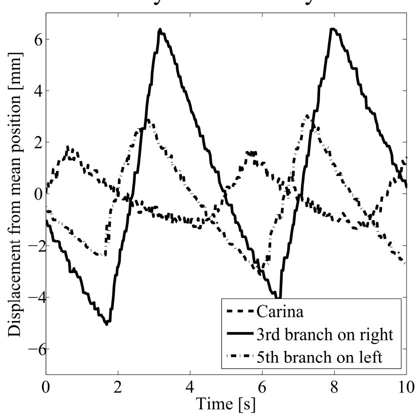

Fig. 8. Displacement of senor with time due to breathing cycle. The sensor was positioned in three positions, one at the carina, a second at a central location in the long and finally at a distal point. The max amplitude of displacement recorded was observed in the centre of the lung.

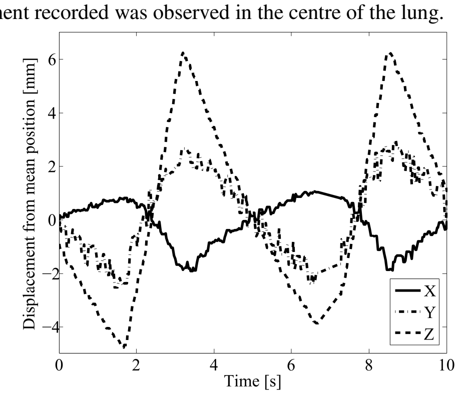

Fig. 9. Individual vector component displacement of senor with time when positioned at a central location in the lung. Maximum displacement is observed in the Z direction. which in this case is vertical.

V. CONCLUSION AND FUTURE WORK

A highly accurate magnetic position tracking system has been presented and evaluated in a breathing lung model. After registration, the majority of recorded points were found to lie inside the boundaries of the 3D lung model. This was confirmed visually with real time display of the sensor probe position. This, in combination with the previously demonstrated accuracy of the system from bench-top tests effectively verifies the overall system operation in the in vitro setting. It was also observed that the close proximity of the probe to the bronchoscope had no observable effect on the system performance.

This planar emitter can be manufactured at low cost due to the PCB coil construction and can easily be extended to operate over a larger working volume. Future designs will use a single PCB board for the entire emitter and will include magnetic shielding to reduce the effect of ferromagnetic materials below the emitter.

The breathing functionality demonstrated will be used for future development of algorithms to counteract the effects of breathing motion on position accuracy and improved registration methodology. This system can then be used for the testing of a virtual bronchoscopy system for peripheral lung biopsy prior to pre-clinical animal trials.

REFERENCES

[1] R. Eberhardt, D. Anantham, F. Herth, D. Feller-Kopman, and A. Ernst, "Electromagnetic navigation diagnostic bronchoscopy in peripheral lung lesions.," *Chest*, vol. 131, no. 6, pp. 1800–5, Jun. 2007.

[2] H. Zhang, F. Banovac, R. Lin, N. Glossop, B. J. Wood, D. Lindisch, E. Levy, and K. Cleary, "Electromagnetic tracking for abdominal interventions in computer aided surgery," Jan. 2010.

[3] A. Plotkin, O. Shafrir, E. Paperno, and D. M. Kaplan, "Magnetic eye tracking: a new approach employing a planar transmitter.," *IEEE Transactions on Bio-medical Engineering*, vol. 57, no. 5, pp. 1209–15, May 2010.

[4] C. Hu, M. Li, S. Song, W. Yang, R. Zhang, and M. Q.-H. Meng, "A Cubic 3-Axis Magnetic Sensor Array for Wirelessly Tracking Magnet Position and Orientation," *IEEE Sensors Journal*, vol. 10, no. 5, pp. 903–913, May 2010.

[5] K. O'Donoghue, P. Cantillon Murphy, D. Eustace, J. Griffiths, H. Mansfield, T. Power, and M. O'Shea, "Catheter position tracking system using planar magnetics and closed loop current control," *IEEE Transactions on Magnetics*, vol. PP, no. 99, pp. 1–1, 2014.

[6] P. Nardelli, R. San Jose Estepar, and P. Cantillon-Murphy, "Semi-automated Airway Segmentation for Lung CT Datasets," in *27th International Congress and Exhibition in Computer Assisted Radiology and Surgery (CARS)*, 2013.

[7] S. B. Solomon, P. White, C. M. Wiener, J. B. Orens, and K. P. Wang, "Three-dimensional CT-guided bronchoscopy with a real-time electromagnetic position sensor: a comparison of two image registration methods.," *Chest*, vol. 118, no. 6, pp. 1783–7, Dec. 2000.

[8] S. X. Liu, L. F. Gutiérrez, and D. Stanton, "Quantitative evaluation for accumulative calibration error and video-CT registration errors in electromagnetic-tracked endoscopy.," *International journal of computer assisted radiology and surgery*, vol. 6, no. 3, pp. 407–19, May 2011.

[9] D. Deguchi, K. Ishitani, T. Kitasaka, K. Mori, Y. Suenaga, H. Takabatake, M. Mori, and H. Natori, "A method for bronchoscope tracking using position sensor without fiducial markers," in *Medical Imaging*, 2007, p. 65110N–65110N–12.

[10] T. Klein, J. Traub, H. Hautmann, A. Ahmadian, and N. Navab, "Fiducial-free registration procedure for navigated bronchoscopy.," *Medical image computing and computer-assisted intervention : MICCAI ... International Conference on Medical Image Computing and Computer-Assisted Intervention*, vol. 10, no. Pt 1, pp. 475–82, Jan. 2007.

[11] C. Nafis, V. Jensen, and R. Von Jako, "Method for evaluating compatibility of commercial Electromagnetic (EM) micro sensor tracking systems with surgical and imaging tables," in *Proceedings of SPIE*, 2008.

[12] D. Ruan, J. A. Fessler, and J. M. Balter, "Mean position tracking of respiratory motion.," *Medical physics*, vol. 35, no. 2, pp. 782–92, Feb. 2008.

[13] Y. Seppenwoolde, H. Shirato, K. Kitamura, S. Shimizu, M. van Herk, J. V. Lebesque, and K. Miyasaka, "Precise and real-time measurement of 3D tumor motion in lung due to breathing and heartbeat, measured during radiotherapy," *International Journal of Radiation Oncology*Biology*Physics*, vol. 53, no. 4, pp. 822–834, Jul. 2002.